Secondary electron emission of carbonaceous dust particles

I. Stefanović,[1,2,*] J. Berndt,[1] D. Marić,[2] V. Šamara,[2] M. Radmilović-Radjenović,[2] Z. Lj. Petrović,[2] E. Kovačević ,[1] and J. Winter[1]

[1]*Institute for Experimental Physics II, Ruhr-University Bochum, D-44780 Bochum, Germany*

[2]*Institute of Physics, Pregrevica 118, 11080 Belgrade, Serbia*

(Received 9 March 2006; published 31 August 2006)

In this paper we present measurements of the secondary electron emission yield (γ) of a carbonaceous dust particle material, which was grown in argon diluted acetylene plasmas. One aim was to reach a better understanding of charging and discharging processes of dust particles in complex plasmas due to secondary electron emission and consequently to try to explain the anomalous behavior of electron density observed in afterglows of pulsed rf plasmas. We compared the results of a simple model and of a Monte Carlo simulation to the previously measured time dependence of the electron density in complex plasma afterglow. It was found that the value of the intrinsic secondary electron yield from the carbonaceous dust material is too low to explain the increase of electron density in the afterglow. It is, however, possible that the electrons charging the particles are weakly attached so that they may be released with high efficiency by ion bombardment due to field induced emission or by other mechanisms.

DOI: 10.1103/PhysRevE.74.026406 PACS number(s): 52.25.Tx, 52.27.Lw, 52.40.Hf, 52.80.Dy

I. INTRODUCTION

Dust formation and growth in low temperature plasmas [1,2], structure formation [3], and the astrophysical importance of the dust in interstellar media (ISM) [4] were extensively analyzed in the last decade. Numerous properties of dusty plasmas and dust particles were discussed, such as the formation and growth of particles [5–10], particle density, size and refractive index [11–14], their influence on the plasma properties [15,16], the buildup of strongly coupled systems such as plasma crystals [17–19], the formation of a void and vortices [20], the wave propagation and interactions in dusty plasmas [3]. Some of the experiments with dusty plasmas were made under microgravity conditions in parabolic flight experiments [21,22] or in the ISS space station [23]. It is generally accepted that the dust particles charging and discharging in plasmas plays an important role in the dynamics and transport properties of laboratory and space plasmas. Depending on the plasma conditions the particle charge can be either positive or negative [24], but usually the dust particles in laboratory plasmas are negatively charged.

Charging of dust particles in plasmas is often described by orbital-motion-limited (OML) theory that balances positive ion and negative electron fluxes to the particle [25]. OML theory originates from the plasma probe theory which describes charging properties of a floating sphere immersed in plasma [26]. The OML theory usually overestimates the charge of a single dust particle [27]. One of the reasons for the discrepancy between the measured and calculated particle charges could be due to an often made assumption that the effect of the secondary electron emission from the dust surface may be neglected. On the other hand, for dust in astrophysical environments different charging mechanisms have been treated, including photoelectric emission and field emission of electrons and positive ions [28]. Still, there were only a few studies of the role of secondary electron emission from the dust particles in the plasma and its effect on the overall charge balance of the dust particles and in the plasma [21,24,29].

Recently, pulsed operation of rf plasmas with a large number of submicron dust particles was studied [30]. It was found that in the afterglow the electron number density first increases before it starts decreasing [30]. The most likely sources of the increased electron density are negatively charged dust particles that may (as has been postulated here) release electrons in the afterglow by the secondary emission.

Possible sources of secondary electron emissions in partially ionized plasma are collisions of electrons, ions, or fast neutrals with gas molecules and surfaces, gas phase and surface collisions of metastables and photoemission due to UV radiation. All of these processes were shown to be important for the breakdown conditions in parallel plate geometries and for relatively low pressures [31] corresponding to the conditions found in our radio-frequency (rf) plasma device [30,32,33].

However, we know very little about some of the basic properties of the particles, especially the secondary electron emission yield (γ) of the material that constitutes dust particles. Data exist for graphite but not for the carbon deposited from the plasma, which has a cauliflower structure of the surface [32–34]. In this paper we present measurements of the secondary electron yield of the dust particles material for the conditions of a gas breakdown. It was shown in the literature that in modeling of the breakdown data (Paschen curves) [31] one needs to combine secondary emission of not only ions but also of other particles such as photons and metastables and fast neutrals and also to include electron back diffusion and other nonequilibrium (nonhydrodynamic) effects close to the surfaces. The intrinsic effective secondary electron emission yield for the dust particle material was thus determined from the measured breakdown curves by applying the Townsend breakdown condition. Based on the previ-

*Corresponding author. Electronic address: Ilija.Stefanovic@rub.de

ously proposed mechanism [30] we develop a simple hydrodynamic model to explain qualitatively the anomalous behavior of the electron density in the dusty plasma afterglow [30] (i.e., the increase of the electron density shortly after the beginning of the afterglow-plasma off period). We discuss possible sources of the increase of the electron density in the early afterglow. We also present a Monte Carlo model that traces the trajectories of the ions and electrons in the vicinity of the particles in an attempt to model charge kinetics of the dust particles in the afterglow.

II. EXPERIMENTAL SETUP

We made a two stage experiment in order to measure the secondary electron yield of the dust particles. During the first phase we generated thin films of the dust particle material on stainless steel or copper substrates. In the second phase we used these substrates as cathodes of a separate pulsed dc low pressure breakdown experiment. In that experiment low current discharge volt-ampere characteristics were measured and extrapolated to zero current.

A. Generating the thin film of the dust particle material and collecting the particles

The dust particles were formed in capacitively coupled rf plasma through plasma polymerization of acetylene monomer diluted in argon [32,35]. The capacitively coupled parallel plane electrode discharge was connected to a 13.56-MHz rf power source. The standard applied power was 15 W. Continuous flow of the argon and acetylene gas mixture, with 8:0.5 cubic centimeter per minute at standard temperature (SCCM) flow ratio, was fed into the discharge chamber and the pressure was kept at 0.1 mbar. We could trace the particle growth and measure the plasma properties with various diagnostics, such as laser light scattering (LLS), Fourier transformed infrared (FTIR) spectroscopy, plasma ion mass spectroscopy, and light emission spectroscopy [32,35]. Dust particles and thin films of the dust particle material were deposited on stainless steel or copper plates, 45 mm in diameter. It was shown that the entire surface was coated. We were able to deposit either smooth films or films with dust particles incorporated in the film. Both of these surfaces were used later for the secondary electron yield measurements. The size of the deposited, monodisperse particles was controlled by the discharge running time, with the previously measured particle growth rate [33]. More details of the experimental setup and diagnostics could be found in Refs. [32–34].

Measurements of the pulsed plasma behavior (electron number density) were performed in the same experimental device which was described in Ref. [30]. Dust particles were formed and then acetylene flow was turned off. During the "plasma off" period, losses of the dust particles were relatively small so the dust plasma structure was recovered in the "plasma on" period. Some observations of the increase of the electron density in the afterglow were made in pure argon but best observations were made when some acetylene was present. Electron number density was measured by a microwave interferometer [30].

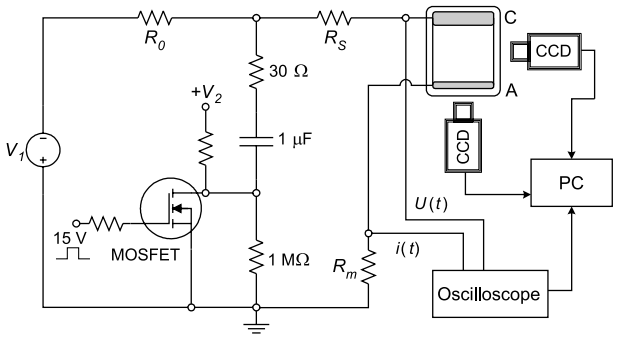

FIG. 1. Simplified schematics of the experimental setup and the electrical circuit for measuring the secondary electron yield.

B. Measuring the secondary electron emission yield (γ)

Secondary electron emission yield was determined by using a pulsed Townsend discharge extrapolated to zero current and Paschen law. We did not rely on independent measurements of ionization coefficients but we determined the effective multiplication from the spatial emission profiles [31,36].

The schematic of the experimental setup (described in our previous papers, e.g., Ref. [37]) is shown in Fig. 1. The discharge operates in a parallel plane electrode system and it is confined within a quartz cylinder that prevents the long-path breakdown. Three sets of measurements were carried out, with three different cathode surfaces (C): (i) stainless steel cathode, (ii) thin film of the dust particle material deposited on the stainless steel electrode, and (iii) dust particles and thin film deposited on the stainless steel electrode. As a test we also used copper substrates and additional measurements were made with a copper electrode and a copper covered with the amorphous carbon film. The anode (A) is made of quartz with a transparent yet conductive thin film of platinum deposited on its surface facing the discharge. The effective (the diameter facing the discharge) diameter of the electrodes ($2r$) is 4.2 cm while the electrode separation (d) is 1.8 cm. The system was pumped down to a base pressure of the order of 10^{-6} mbar before being filled by argon. The operating pressure is maintained by using a very small flow of pure argon.

The discharge voltage measurements are carried out in a pulsed regime, in order to avoid significant conditioning of the cathode surface [37,38], which is especially critical when a thin film of dust particles is coated on the cathode. Repeated measurements confirmed that the results are stable and reproducible. The discharge current of the dc Townsend discharge was limited to 0.5–1.0 μA and from those values it was pulsed to higher currents.

At the same time, the axial intensity profiles were recorded by an ICCD camera (Andor IStar DH720-18U-03). Pulses of currents lasted long enough to make reliable recordings of the spatial profiles of emission and of the discharge maintenance voltage so that the emission profiles correspond to the conditions of the pulse (50 ms). Besides the electrical measurements and the axial emission profiles, we can also measure the radial profiles of emission through the transparent anode electrode. While we do not measure absolute values of the emission intensities, the relative relation-

ship between the emission profiles at different currents is maintained. In principle, it is possible to make absolute calibration of all the data by normalizing the profiles in the low current Townsend regime to the excitation coefficients at the anode.

C. Procedure for determination of $\gamma(E/N)$

The procedure used to determine $\gamma(E/N)$ data from the breakdown voltages and low-current discharge characteristics is based on Townsend breakdown (self-sustaining) condition:

$$\gamma = \frac{1}{\exp\left[\frac{\alpha}{N}\left(\frac{E}{N}\right) \times N(d - d_0)\right] - 1}, \tag{1}$$

where α is the Townsend ionization coefficient, E is the electric field, N is the gas particles number density, d is the electrode separation, and d_0 is the length of nonhydrodynamic region close to the cathode. The exponential term is actually equal to the electron multiplication factor. The procedure was described in detail in Refs. [31,36].

Our experimental setup enables the measurement of the maintenance voltage for low-current discharges in a relatively broad range of pressure times electrode gap (pd) products (Paschen curve). However, we confine ourselves to the values around the Paschen minimum and to the left of it because that is the range relevant (in terms of mean electron energies and energies of ions hitting the surface) to model conditions in realistic capacitively coupled plasmas used for generating dust particles and for thin film deposition. In the low current limit of the discharge, the electric field is assumed to be homogeneous ($E=V/d$). Ionization coefficients $\alpha(E/N)$ are determined directly from the experimentally recorded spatial profiles of emission by fitting the emission profile. Exponential increase of the emission intensity from the cathode towards the anode is assumed for the hydrodynamic region which is typical for homogeneous field conditions in the low-current Townsend discharges.

It should be noted that because of the specific geometry of the discharge chamber, we were not able to determine accurately the width of the nonequilibrium region near the cathode. This could lead to a possible overestimation of the electron multiplication, i.e., underestimation of the secondary electron emission [31,36]. The delay or equilibration distance (d_0) is given as $d_0=V_0/E$, where V_0 was calculated with the semiempirical formula proposed by Phelps and Petrović [31,39–41]:

$$V_0 = 16\sqrt{1 + \left(\frac{E/N}{1000}\right)^2}. \tag{2}$$

Here V_0 is potential difference required before the discharge current begins to grow exponentially and is in volts, whereas E/N is in Td. The semiempirical formula (2) proved to be in excellent agreement with the Monte Carlo calculations and experimental measurements of the d_0 for the case of argon [41]. Thus the effective growth of electron number density was obtained by subtracting the nonequilibrium region from the discharge gap and allowing further growth determined from the slope of emission. Nevertheless, the effective ionization coefficients were shown to be in a reasonable agreement with the accepted data [36].

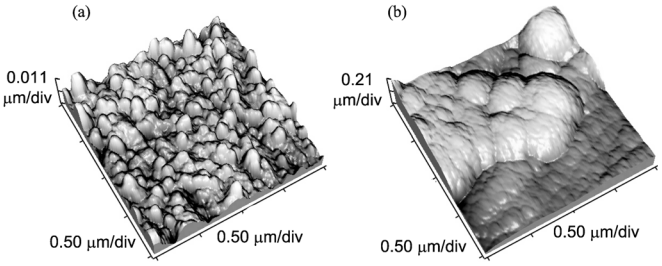

FIG. 2. Atomic force microscope scans of different polymer surfaces: (a) film, (b) film with embedded particles. The vertical scale at (b) is about 20 times larger than at (a).

III. EXPERIMENTAL RESULTS

We measured the surface morphology of the thin film and the thin film with the particles by the use of atomic force microscopy [Figs. 2(a) and 2(b)]. The roughness of deposits differs by one order of magnitude. The particles were deposited to the film when their diameter was expected to be around 200 nm, which was confirmed separately by an electron microscope [33]. The morphology of the thin film covering the cathode was expected to affect the breakdown condition in the gas. It may be argued that the film deposited on the electrode will be different in compactness and morphology to that of the particles which are created under somewhat different conditions.

In Fig. 3 we show Paschen curves for three different cathode surfaces: stainless steel (squares), stainless steel covered by a layer of dust particles suspended in film made of the dust particle material (circles), and finally the stainless steel covered only by polymer film (triangles), i.e., without depos-

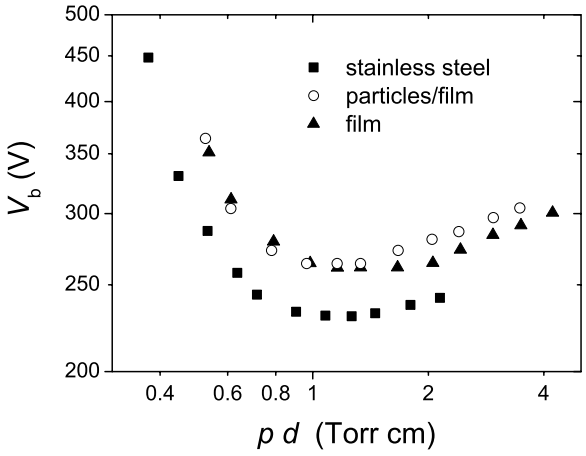

FIG. 3. Paschen curves for three different cathode surfaces: stainless steel cathode (squares), dust/film deposited on stainless steel (opened circles), and film deposited on stainless steel electrode (triangles). V_b describes the breakdown voltage and pd the product of pressure and electrode separation.

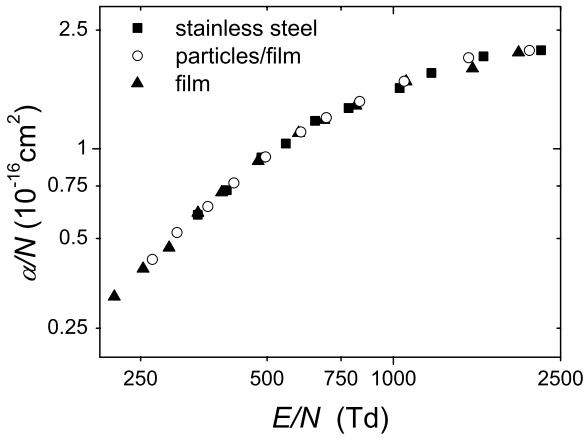

FIG. 4. Ionization coefficient (α/N) upon reduced electric field strength (E/N) in argon, obtained in measurements with different cathode surfaces.

ited dust particles. It is clear that deposited layers of polymer material lead to higher breakdown voltages.

In Fig. 4 ionization coefficients α/N obtained by fitting of experimental axial emission profiles are shown as a function of reduced electric field E/N. As expected, since all the measurements were made in the same working gas (argon), agreement between results obtained with different cathode surfaces is excellent.

Finally the dependence of the γ coefficient on the reduced electric field (E/N), that is derived from the Paschen curves and profiles of emission, for the three cathode surfaces is shown in Fig. 5. The secondary yield for the polymer material is lower than that for pure stainless steel. The increase of γ at low E/N indicates the importance of UV emission [31] and will lead to yields above 1 for very small mean electron energies in plasma. This may appear to correspond to the afterglow conditions, as very high secondary yields are required to reproduce the effect that was observed by Berndt *et al.* [30]. However, the increase of the yield at low E/N occurs due to the requirement to achieve the breakdown (so it is a much higher E/N than the one that we have in the afterglow) and then the photons will participate in the release

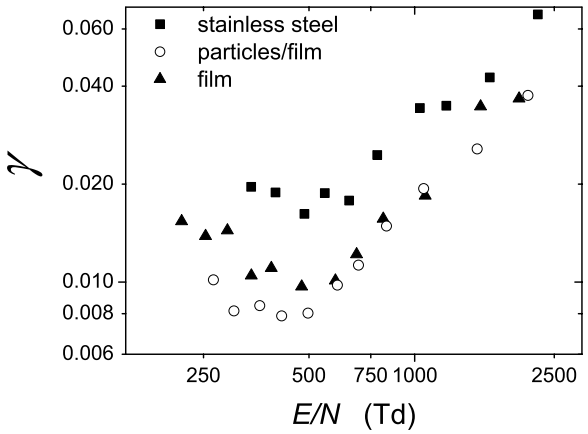

FIG. 5. Secondary electron emission yield γ as a function of the normalized electric field strength E/N for stainless steel, stainless steel covered by dust particles/film, and for film without particles.

of electrons. In the afterglow, while some photons may still be present, their flux will be reduced since electron energies drop down very quickly after the electric field is turned off. Some amount of energy will be stored in argon metastables that may maintain the electron energy at a higher level but in any case the same relationship between the electron flux and the photon flux as for the breakdown conditions will not hold.

It is, however, interesting to note that the main differences between the three materials occur for the breakdown conditions at low E/N or at high pd values where photon induced electron emission dominates [31]. That means that the photoemission is reduced for the surfaces with the polymer coating, and even more for the surfaces with the particles incorporated in the thin film at the surface.

As for the different morphologies of a carbonaceous surface, we can see that breakdown voltages are increased for the surface containing dust particles in the right-hand branch of the Paschen curve. The two surfaces with deposited carbon material behave rather similarly in the left-hand branch. It is important to note that we have made measurements with several different samples of polymer coatings, deposited under different operating conditions. While there are some variations in breakdown voltages, the trends shown in Fig. 3 still remain the same.

One might expect at a first glance the particles at the surface to cause (sub)micron roughness leading to a somewhat higher local field and through field emission to a lower breakdown potential. This is clearly contrary to the observation. We thus conclude that the surface morphology induced by the deposited dust particles does not yield a field increase sufficient to reduce the breakdown voltage, if anything the effect is reverse and it occurs at conditions when fields are likely to be smaller. It actually occurs in the region where there is a large probability that emitted electrons will not reach the discharge due to reflection back to the cathode which is the result of collisions with gas known as back diffusion [42]. The more complex structure of the film due to the presence of the particles will certainly lead to a lower value of the escape probability for electrons from the surface and consequently to lower yields. However, it is not obvious whether the difference between the metallic and the coated surfaces may be explained in the same fashion.

First, it is possible that the lower secondary yield is an intrinsic property of the deposited material but it may also be due to rougher (cauliflowerlike) structure of its surface. The fact that the difference extends to higher E/N perhaps supports more the former conclusion but does not rule out the latter one altogether. The main finding is that quite opposite to our expectations, much too low values of γ were found as to explain the observed anomaly [30].

The results for γ in case of copper cathode and copper covered by the thin film are presented in Fig. 6, together with the results for the stainless steel. There is a good agreement between γ measured for the thin film deposited on different substrates while there is a considerable difference between the results for different metallic electrodes. This indicates that the type of the substrate does not influence the γ values, which underlines the reliability of our procedure.

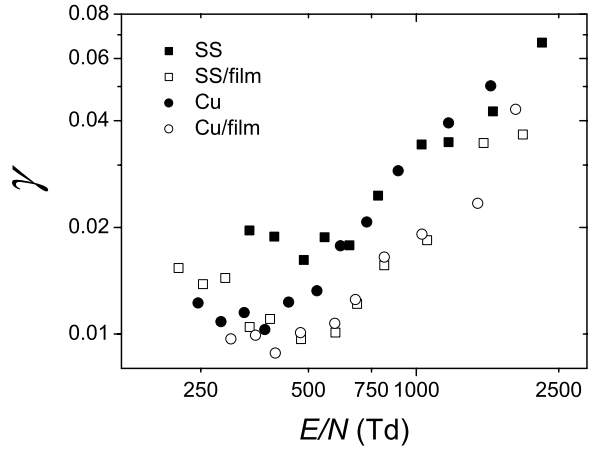

FIG. 6. Secondary electron yields for different cathode material: stainless steel (SS), stainless steel covered with film (SS/film), copper (Cu), copper covered with film (Cu/film).

IV. INCREASE OF ELECTRON DENSITY IN THE DUSTY PLASMA AFTERGLOW

To reach a better understanding of the unexpected behavior of the electron density in the plasma afterglow observed in rf-pulsed plasma experiment [30], we have attempted to fit the temporal development of the electron density in the afterglow. We followed the scenario proposed in Ref. [30], which was based on the standard orbital motion limited (OML) theory assumptions [25–27]. The flux of electrons consists of the electrons from the plasma reaching the surface and of secondary electrons released by ions hitting the surface. The secondary electrons are accelerated towards the plasma. Thus during the quasi-steady-state conditions in the plasma phase, the actual flux of electrons arriving at the surface has to exceed the ion flux by the flux of the released secondary electrons. The working assumption was that the increase of the electron number density in the afterglow may be explained by the breakdown of the balance of particles reaching the surface of the dust particle as given in the following scenario:

(i) In the steady state plasma a potential is formed around the dust particles which slows down electrons and accelerates ions so that fluxes of positive and negative charges at the surface of the particle are equal. Only higher energy electrons may reach the dust particle and we may estimate the potential drop to be of the order of 10 eV, while the mean energy of electrons is several eV.

(ii) After the external field is turned off, the electron temperature rapidly reaches the ambient gas temperature.

(iii) As a result the electrons will not be able to reach the surface of the charged particle as the sheath potential (which will be maintained for a while until either the particle or the plasma lose their charge) is such that very quickly the flux of electrons to the dust particle will cease.

(iv) As a result there will be an effective neutralization of the charge on the particles due to ions but also there will be an effective release of negative charges by the secondary electron production.

(v) The release of electrons will continue while the sheath voltage of the charged particle will gradually collapse and the particles will lose their charge. Over long time, losses of the charged particles to the walls (and by recombination) will make a significant contribution and eventually the number of free electrons will start to decay.

The ion current to the dust particle in the OML regime, for the Maxwellian ion distribution, has the following form:

$$I_i = \pi r^2 e n_i \nu_{th,i}\left(1 - \frac{eV(r)}{kT_i}\right). \tag{3}$$

For a Boltzmann distribution of the electron density the electron current to the dust particle is given through

$$I_e = \pi r^2 e n_e \nu_{th,e} \exp\left(\frac{eV(r)}{kT_e}\right), \tag{4}$$

where $n_{i,e}$ are the ion and electron density of the unperturbated plasma, $T_{i,e}$ are the ion and electron temperatures, $V(r)$ is the dust particle floating potential, r is the particle radius, e is the absolute value of the elementary charge, and $\nu_{th,i,e}$ are the ion and electron thermal velocities,

$$\nu_{th,i,e} = \left(\frac{8kT_{i,e}}{\pi m_{i,e}}\right)^{1/2}.$$

The particle charge and the particle floating potential are related through the following relation:

$$Q = 4\pi\varepsilon_0 r V(r). \tag{5}$$

Dust particles immersed in plasma charge up according to the law

$$\frac{dQ}{dt} = (I_i - I_e) + I_e^{free}, \tag{6}$$

that was modified by the factor I_e^{free}, which stands for the current of (free) electrons leaving the particles, as proposed by Berndt *et al.* [30].

The changes in n_e and n_i in the plasma afterglow are governed by recombination losses on the dust particles:

$$e\frac{dn_e}{dt} = -I_e n_d + I_e^{free} n_d, \tag{7}$$

$$e\frac{dn_i}{dt} = -I_i n_d. \tag{8}$$

In principle, several different mechanisms could explain the release of electrons from the particles, for example: secondary electron emission due to the impact of electrons, ions, UV photons, metastable atoms, and fast neutrals or effects like termionic emission or field emission. In the experimental part of our paper we discussed all relevant collision processes that could produce the secondary electrons under standard breakdown conditions. Some of these effects are less probable in the plasma afterglow such as secondary electron emission due to the electron impact or the photoeffect. As already postulated one could expect that in the plasma afterglow the sheath voltage of the charged particle will gradually collapse. However, the fact that the dust structure is maintained during the afterglow and even when gas mixture is replaced by pure argon means that sufficient charge remains

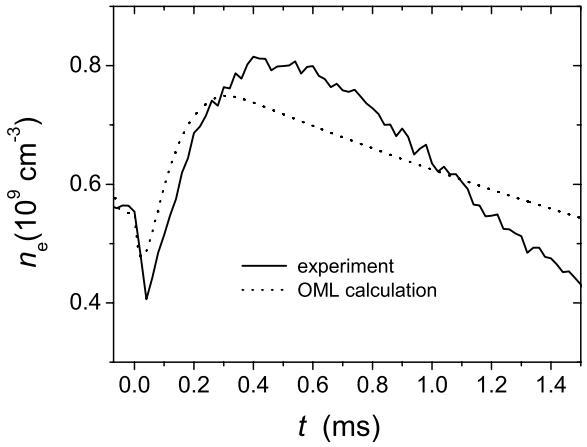

FIG. 7. Electron number density calculated from the model based on the OML theory and the experimental results. The OML calculation was obtained for $\gamma=1$ and the initial mean energy of electrons is 2.15 eV, while the relaxation time for the electron temperature is 50 μs. The particle radius used for calculations is $r=100$ nm and the number of charges is $211e$.

on the dust particles and also that the field around dust particles is maintained. Thus the ions, even though starting with a thermal energy as they enter the sheath around dust particles, will attain high kinetic energy and will be able to release electrons from the dust particles. Thus the current of electrons that are leaving the particle is proportional to the ion current and is given by

$$I_e^{free} = \gamma I_i, \tag{9}$$

where γ is the secondary electron yield. The γ coefficient could be used as the effective secondary electron emission yield that includes all possible processes for liberating the electrons, normalized to the ion current [31].

However, some assumptions had to be introduced to make this model work. First, the time scale for the collapse of plasma should be significantly longer than the thermalization time, second, the value of the time constant for the relaxation of the electron energy in afterglow is assumed, and finally the secondary electron yield has been used as a fitting parameter.

The solution of the system of equations (1) and (7) is presented on Fig. 7, together with the experimental results for the time behavior of the electron density in afterglow. The measured values for the ion and dust particle density were $n_e=1.5\times10^{15}$ m^{-3} and $n_d=4.5\times10^{12}$ m^{-3}, respectively. In calculations we have used general conditions estimated for typical dusty plasmas found in our experiment. The estimated electron temperature kT_e for our plasma conditions was a few eV but in the case shown in Fig. 7 the mean electron energy in the on period of the plasma is 2.15 eV or greater. From the independent particle growth-rate measurements a typical particle radius was estimated at $r=100$ nm [33] and this value was used in our further calculations unless specified separately. For these particles it is estimated from the OML theory that the number of charges is about 211 elementary charges, the potential around the charged particle is found to be −3 V.

The qualitative agreement between the experimental results for the electron density in the afterglow and calculated ones are excellent for $\gamma=1$. It was observed that the shape of the first minimum depends strongly on the relaxation time of the electron temperature and the best results were observed for $\tau=50$ μs, where τ is the time constant of the electron energy relaxation and $T_e=T_{e,0}\exp(-t/\tau)$. The relaxation time constant was used as one of the fitting parameters. In this specific case the best value was within ±30%.

In a separate code (see Ref. [43]) we have studied the relaxation kinetics of the electron energy in the argon plasma afterglow, for the conditions similar to those in the experiment (pressure 50 mTorr, initial energy distribution function was a Maxwellian with 2.15 eV mean energy in pure argon). The idea was to test whether selected values of thermalization times are realistic. In the first experiment [30] we grew the dust particles in the argon-acetylene mixture and when they reached a certain size we switched off the acetylene, to prevent particles from growing further. It took several minutes to replace all the acetylene with argon so we may claim that the experiments were performed in pure argon with significant contamination of acetylene. During the off period some charges were lost and were replaced by the charging in the on period. However, some particles would be lost from the plasma and we could not extend the experiments any beyond several minutes due to particle losses in the off period. Our pulsed experiment was therefore performed on the plasma constituting of the dust particles and essentially of argon as a background gas though best results were obtained when there was some acetylene still in. While the thermalization of electrons in pure argon is relatively slow, the high energy tail gets depleted very quickly due to inelastic processes above 11 eV (see Ref. [44], Fig. 6.8, for a review of thermalization times as a function of the mean electron energy). The typical time constants for the electrons with energies above 3 eV are of the order of less than 100 ms as energy increases due to a high cross section for elastic scattering. However, below 1 eV the relaxation times increase by more than three orders of magnitude. The high energy tail coincides with the group of electrons that may arrive at the surface of the particle, which is floating at a potential of 3 V required to equate the fluxes of ions and electrons. These values of the relaxation times were confirmed by our Monte Carlo simulations more directly. While thermalization times for the bulk electrons below the threshold for excitation are quite long, the times required to thermalize the high energy tail of electrons for the same pressures as used in the experiment, were quite short and consistent with the relaxation times found to fit the experimental data best. A small amount of acetylene, that was expected to be present, helped speed the relaxation at energies below 11 eV.

In the Fig. 7 one can see that after the first minimum the electron density increases. The subsequent decay of the electron density is observed only due to the discharging of the particle, thus the losses of electrons to the walls by diffusion or due to gas phase recombination were not taken into account. As a result our calculated dependence is in slight disagreement with the experiment at later times probably due to

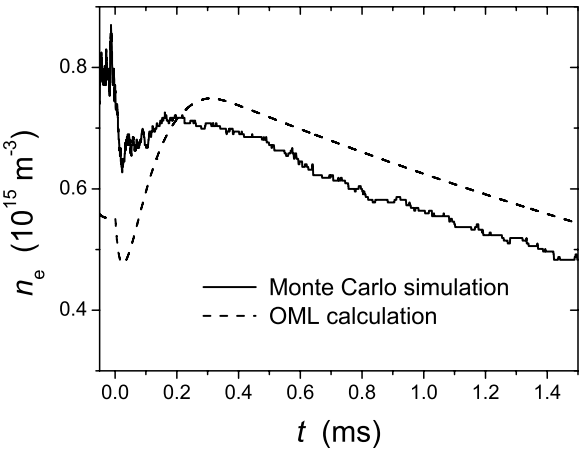

FIG. 8. Comparison of OML and Monte Carlo approach for the same general conditions as in Fig. 7.

the complex diffusion mechanism involved during plasma neutralization.

We may conclude that previously proposed mechanism of the anomalous electron density behavior in plasma afterglow gives the right time dependence of electron density if the secondary electron yield is sufficiently large and the electron energy decay is sufficiently fast.

Finally, we have tried to implement a full Monte Carlo simulation as a test of the OML calculation. The initial conditions were the same as in the previous calculation. Electrons and ions were released in the region of a particle and their trajectories were tracked in the field induced by the charges on the particle. If an ion hits the particle $(1+\gamma)e$ was added to its charge (here e is positive) and if an electron hit the surface $1e$ was subtracted. This approach is similar to that of Cui and Goree [45]. The results of the Monte Carlo simulations are shown in Fig. 8 parallel with the OML calculations. Subject to a large statistical uncertainty Monte Carlo results were fully consistent with the OML calculations.

To conclude, we may say that it was possible to find a phenomenological explanation to the afterglow dependence of the electron number density. However, the required secondary electron yield, for reasonable thermalization times, is in disagreement with the yield obtained from the Paschen breakdown law for the same material as measured in our experiment. Thus the property of the material itself cannot explain the high efficiency of the release of electrons in the afterglow. In other words, high secondary emission is not an intrinsic property of carbonaceous material that constitutes the dust particles.

V. POSSIBLE EXPLANATION OF THE HIGH SECONDARY ELECTRON YIELDS IN THE DUSTY PLASMA AFTERGLOW

To conclude, we have found that it is possible to describe the increase of the electron number density in the plasma afterglow if we check the balance of charges during the thermalization of electrons. The results of the model depend both on the value of the secondary electron yield and on thermalization time. In the following section we shall discuss whether the high values of secondary electron yield are feasible in the plasma afterglow.

It is of course difficult to make a comparison between the results of our experiment obtained from the breakdown study and the conditions in the afterglow plasma experiment, as the conditions are not really the same. In the former case the field is high but initially there are no excited species or ions. As discussed by numerous authors the effective secondary yield for breakdown at low fields is typically very high (above 1) [31] due to the effect of resonant photons. The external electric field is zero in the latter case but there is a large number of initial ions, electrons, and excited particles that are left over from the plasma. While some effect of the photons may exist in the initial stages (typically of the order of the effective lifetime of excited states) the effect of photons will soon disappear. In addition, the area of the particles is also very small compared to the area of the sheath around them or compared to the electrodes even for the trapped resonant radiation so the effect of photons in our case would be smaller than that in the parallel plate breakdown.

From the modeling of our experimental results for the γ of the carbonatious dust particle material we may conclude that the source of electrons that are released must be associated with some more efficient mechanism of secondary electron emission. The first possibility that comes to mind is the electric field induced emission. This idea was inspired by the importance of the field emission in breakdown for very small gaps (of the order of few micrometers; for example, see Ref. [46]). There was also some effort to estimate the contribution of field emission processes on the charge distribution for small particles [28]. The field around the particles appears to be too weak to produce significant emission on its own. Thus we have postulated that there could be a transient effect of the field between the ions and the particles. As ions approach the particle they may induce a very large transient field even if they miss the particle. On the other hand the duration of the close encounters is very short. Field emission effect due to the ion induced transient field should be important at a distance larger than the typical distance where Auger process becomes effective. The process could be facilitated by a large external field as suggested in Ref. [47].

It is important to note that here we just try to show feasibility of such a proposal. The test will be carried further showing which possible mechanisms may contribute to the high values of the secondary yield without actually making a claim that we have a proof of a particular mechanism.

A. Electron current induced by transient field effect and γ

The idea that ions may induce emission when they arrive close to the surface of the dust particle even if they do not collide with the particle will be tested further. In addition, the necessary condition is that the released electron does not neutralize the ion, or at least not before other electrons had a chance to be released. It has been suggested [47] that considerable emission may occur by the transient field induced by ion approaching a surface provided that an external field

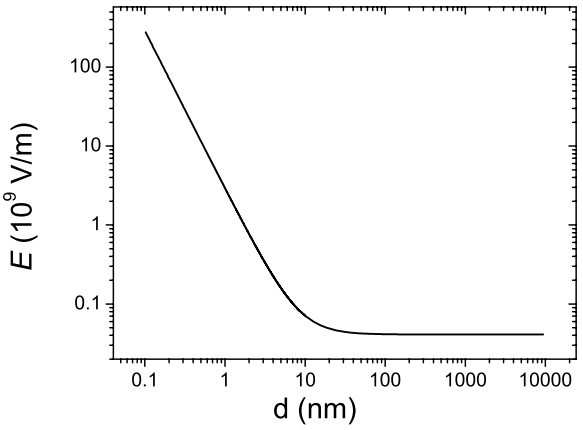

FIG. 9. Calculated electric field at the particle surface induced by the approaching ion.

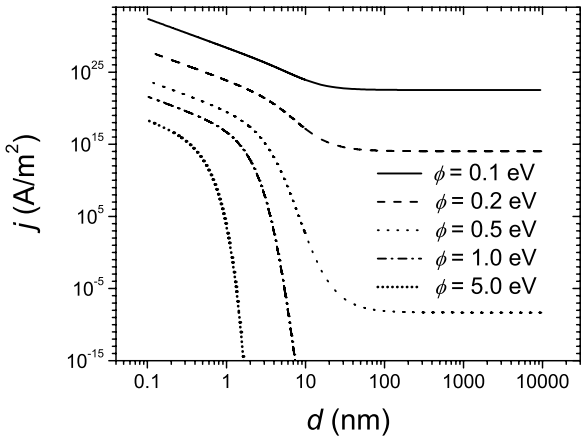

FIG. 10. Electron current density induced by field emission effect upon the ion-particle distance. As a parameter the different values of electron bonding energy (work function) is shown.

exists that may facilitate the release of emitted electrons without neutralization of the ion. In order to determine the effective γ as a result of these assumptions we made simulation of Ar^+ ions approaching the negatively charged dust particle of a spherical shape. We wanted first to test whether the approaching Ar^+ ion can produce an electric field on the surface of the particle strong enough to induce field emission and if so under which circumstances would it be sufficient to explain the experimental data. In our simulation the an ion can induce the transient field and the corresponding field emission but may also produce the secondary electrons through the Auger process if it collides with the surface. While basic theories of binary collision experiments [48] allow estimates of the yields for potential secondary emission that would be relevant for binary experiments. We have, however, used our estimates of the yields from the analysis of the Paschen curves for moderate energies.

To calculate the field strength induced by an ion on the particle surface the classical electrodynamics image method was used. The field on the particle surface depends on the ion-particle distance as it is shown in Fig. 9 and the enhancement of the field becomes significant for distances of less than 10 nm. One should remember that a sufficiently strong external field is required to make it possible for the emitted electrons to escape the ion.

To estimate the electron current from the dust particle emitted through the field-emission effect the Fowler-Nordheim formula was employed [49] (since the Fowler-Nordheim equation usually predicts to low emission for a given field strength as compared to the experiments [49] we may expect the emitted currents to be even higher than predictions shown here):

$$j_F = \frac{1.54 \times 10^{-6} \times 10^{4.52\phi^{-0.5}} E^2}{\phi} \exp\left\{-\frac{6.53 \times 10^9 \times \phi^{1.5}}{E}\right\}. \tag{10}$$

In this formula j_F stands for the electron current induced by the field emission, E is the electrical field strength on the particle surface and ϕ is the work function of the material. One has to notice that this formula has been developed for the case of metal surfaces and parallel-plane geometry. In Fig. 10 the electron current density as a function of the minimum distance between the approaching ion and the dust particle is shown for different values of the work function ϕ. It can be seen that j_F strongly depends on ϕ and that the range is such that for some low values of the work function any requirement for the secondary emission may be met.

Trajectories, velocities, and positions of ions were traced in the sheath region of the dust particle by using the Monte Carlo code. The secondary yield was integrated over the trajectories of ions taking into account the time decrements:

$$\gamma = \frac{\int_{d=\infty}^{d=R} I(d)dt}{e}. \tag{11}$$

The result of this simulation is shown in the Fig. 11 as a dependence of the secondary emission yield upon the electron binding energy. For the integration limit we used some minimum distance (d_m) for which the ion can be treated as if

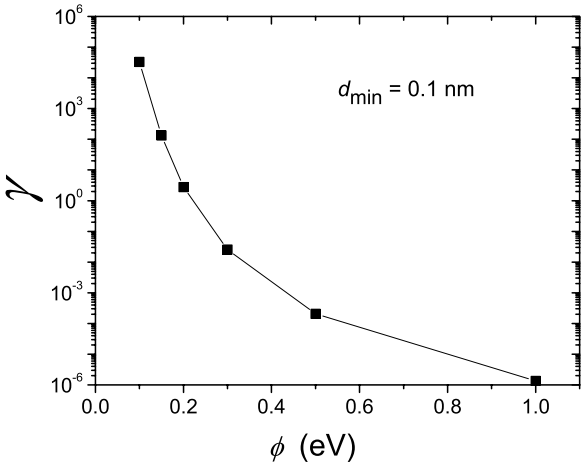

FIG. 11. Calculated γ as a number of electrons released by one ion, over the time required to pass by the dust particle with 0.1 nm as the minimum ion-particle distance.

it did not hit the particle surface. The minimum distance was chosen to be 0.1 nm, which is equal to the estimated diameter of an ion. It is also obvious that the integration should stop at the point when neutralization occurs.

There is a large probability that the electron released can be captured from the incoming ion and thus be neutralized. Newton [47] has shown that a positive ion in a high field ($\sim 10^7$ V/cm) may be able to eject several electrons from a metal surface by tunneling through the barrier between the surface and the ion provided that external field is sufficiently high. He employed a simple calculation to estimate the electron emission in high external electric field. He showed that, depending on the external electric field and the ion distance, the induced electron current can be several orders of magnitude larger than the current induced by the "pure" field emission effect [47].

Our calculations show, however, that the effective secondary yields are not sufficient unless we assume weakly bound excess electrons at the surface (i.e., the electrons are in the weakly bound surface states). Our next assumption is that electrons are bound to the shallow surface states and may be released by a number of effects.

B. Discussion of possible explanations of the high effective secondary electron yields γ

As it can be seen from the Fig. 10 very large yields may be provided depending on the binding energy of the electrons at the dust surface. The issue of the work function or the binding energy for electrons is thus critical. In principle the work function for the carbon material is of the order of 5 eV [50] which is not sufficient to justify the high electron yields found in the dusty plasma afterglow experiment. Thus we postulated that electrons may be weakly bound to the surface of the particle and may be released more easily by the incoming ions. It turns out that, for the binding energies of the order of 0.5 eV and less, the probability of the release of a charge from the surface by the induced transient field will become large. There is at least a good chance that electrons will be released in accordance with the yields required to explain the experimental data.

Observations of the weakly bound electrons have been made in the past. Pavlu and co-workers [29] discussed binding energies of the order of less than 1 eV for materials that should have the binding energies of several eV. On the other hand Robertson and co-workers have studied photoemission induced charging of dust particles for astrophysical conditions [51]. The charging to positive potentials requires the extraction of electrons from the material and thus work functions are expected to be in accordance with the intrinsic properties of the material. Here, however, we discuss discharging of negatively charged particles which are most likely to store the excess charge at the surface or in the levels formed in the forbidden gap due to defects in the crystalline structure, effect of the surface, or impurities [28,52]. Calculations indicate that the excess negative charge stored on a nanosize particle will lead to the reduction of the binding energy, depending on the particle charge and its diameter [28,53]. The evidence of weakly bound charges diffusing over the surface was found in Cavalleri diffusion experiment [54]. Electrostatic force microscopy was used to study the transport of weakly bound charges on a surface of silicon dioxide [55]. This is important to describe the area covered by a single charge and the probabilities that the incoming ion may hit the area that has an extra charge. For thermal emission this issue may not be important. The lifetime of electron in a weakly bound state should also be considered in calculation of the collision probabilities.

One may argue that if weakly bound electrons are present, field induced emission may not even be necessary to explain the high effective secondary electron yields. Under those circumstances one may rely on thermal emission of electrons even at room temperatures. The process of thermal emission from clusters has been studied in Ref. [56] but not from much larger size dust particles, which also store much more negative charges. The thermal emission at the room temperature may yield equally high effective emission of electrons also, provided that the binding energies are of the order of 0.1 eV. In addition, the Auger process with the weakly bound electrons may provide high secondary electron yields and such study is needed in the literature. In Ref. [57] a linear dependence is found on a double logarithmic plot of the potential (Auger) secondary electron emission as a function of $(0.78E_i - 2\phi)$ where E_i is the energy of neutralization of the incoming ion and ϕ is the work function. In the limit of small work functions one may expect yields as high as 0.5. Such secondary electron emission yield is sufficient to provide a very good fit to the experimental data for the electron density in the afterglow, provided that electron energy relaxation is fast enough. This was confirmed by both our calculations and those made by the referee.

In any case (whether field induced or thermal emission or some other mechanisms are used to explain the excess electron emission in the afterglow) all of the proposed processes may be phenomenologically described through the secondary electron yield and may be included in the OML equations. In addition to the mentioned papers [29,51,52] one apparently relevant study has been made on reduction of the charges that are accumulated on satellites orbiting in higher regions of the atmosphere. It has been found that the best way to reduce the extra charges is the emission of positive ions from the surface. In that case ions return to the surface because of the very strong electric field and produce a lot of secondary electrons [58]. This mechanism is, however, efficient for potentials in excess of 1 kV.

VI. CONCLUSION

We have tested a hypothesis that the increase of electron density observed in Ref. [30] may be the result of a standard secondary electron release by ionic bombardment in the afterglow. The model for the time evolution of ion and electron density in the plasma afterglow was developed using the standard OML approach. The results of a simple model qualitatively explain well the experimentally observed electron density increase in the afterglow [30]. An additional Monte Carlo simulation of the dust particle charging and discharging in plasma afterglow supports the results of the model.

We have measured the yields for the surfaces coated by a film of the dust particle material and the surfaces covered by both the particles and a thin film. It was found that these yields are lower than those for standard stainless steels and/or copper and definitely too low to explain the time dependence of the electron density in the afterglow. The measured values for ionization coefficients under different electrode conditions have confirmed the reproducibility and reliability of the measurements. Thin film deposited on the different substrate materials (stainless steel and copper) showed the same γ coefficients and such systems could possibly be used as a cathode material with stable and reproducible characteristics. We have compared the breakdown by using electrodes that had and did not have incorporated dust particles in the deposited thin film and the conclusion is that there was no difference, indicating that the geometry was such that the effect of higher fields at the small size structures did not affect the electron emission.

The very large yields, even of the order of 1, that were observed for the low E/N under breakdown conditions are presumably due to photoemission [31] and thus may not explain the yields in the plasma afterglow.

As a support to one of the possible explanations of the high electron yields found in afterglows seeded with charged dust particles a model for ion and electron motion in the vicinity of the dust particle was developed using Monte Carlo simulation technique for a collisionless sheath. The ion approaching the dust particle was traced and the ion induced electric field on the dust particle surface was calculated as a function of the distance. By using the Fowler-Nordheim formula for field emission we calculated the electron current released from the dust particle during the ion approach to the particle. On this basis the effective γ was calculated with the dust particle work function as a parameter. It was shown that the standard work function is not sufficient to fit the experimental data. Failure to fit the experimental data observed in our experiment by intrinsic properties of the material constituting the dust particles leads to a possible explanation for the increase of the electron density in the dusty plasma afterglow by the release of weakly bound electrons from the surface of the negatively charge particles. If low working function of electrons is invoked to explain the data then one may not need the transient field emission, the effect may be achieved by other means such as the thermal emission of weakly bound electrons even at the room temperature. These processes may be described phenomenologically through the secondary electron yield and employed in the theory. The excess electrons charging the dust particles will spend some time in the shallow surface states. To our knowledge, studies of the Auger emission of secondary electrons with the added effect of the shallow surface states have not been done. Such results would be welcome for explanation of the electron emission from the surface of negatively charged dust particles.

Further studies of the charging of dust particles in the plasma and the binding energy for electrons would be welcome, in particular by using photoemission induced by lasers.

ACKNOWLEDGMENTS

This work was supported partly by Project No. 141025 of the MNZZS of Serbia SFB 591 of Deutsche Forschung Gemeinschaft through SFB 591, Project No. B5. The authors are also grateful to our colleagues from the IHTM institute in Belgrade, Dr. D. Vasiljević and Professor Z. Djurić, who have performed atomic force microscopy measurements of the surface structures of the thin films studied in this paper.

[1] See, for example, *Dusty Plasmas: Physics, Chemistry and Technological Impacts in Plasma Processing*, edited by A. Bouchoule (Wiley, Chichester, 1999); *Focus on Complex (Dusty) Plasmas*, Special Issue of New J. Phys. **5** (2003).
[2] J. Berndt, S. Hong, E. Kovčević, I. Stefanović, and J. Winter, Vacuum **71**, 377 (2002).
[3] P. K. Shukla and A. A. Mamun, *Introduction to Dusty Plasma Physics* (Institute of Physics, Bristol, UK, 2002).
[4] Y. J. Pendleton and L. J. Allamandola, Astrophys. J., Suppl. Ser. **138**, 75 (2002).
[5] A. A. Howling, L. Sansonnens, J.-L. Dorier, and Ch. Hollenstein, J. Phys. D **26**, 1003 (1993).
[6] A. Garscaden, B. N. Ganguly, P. D. Haaland, and J. Williams, Plasma Sources Sci. Technol. **3**, 239 (1994).
[7] J. Perrin, Ch. Bhm, R. Etemadi, and A. lloret, Plasma Sources Sci. Technol. **3**, 252 (1994).
[8] A. Bouchoule and L. Boufendi, Plasma Sources Sci. Technol. **2**, 204 (1993).
[9] E. Stoffels, W. W. Stoffels, G. W. Kroesen, and F. J. de Hoog, J. Vac. Sci. Technol. A **14**, 556 (1996).
[10] U. Kortshagen and U. Bhandarkar, Phys. Rev. E **60**, 887 (1999).
[11] A. A. Howling, Ch. Hollenstein, and P. J. Paris, Appl. Phys. Lett. **59**, 1409 (1990); Ch. Hollenstein, J.-L. Dorier, J. Dutta, L. Sansonnens, and A. A. Howling, Plasma Sources Sci. Technol. **3**, 278 (1994).
[12] D. Samsonov and J. Goree, J. Vac. Sci. Technol. A **17**, 2835 (1998).
[13] K. Tachibana, Y. Hayashi, T. Okuno, and T. Tatsuta, Plasma Sources Sci. Technol. **3**, 314 (1994).
[14] G. Gebauer and J. Winter, New J. Phys. **5**, 38 (2003).
[15] R. N. Carlile and S. Geha, J. Appl. Phys. **73**, 4785 (1993).
[16] Ph. Belenguer, J. Ph. Blondeau, L. Boufendi, M. Toogood, A. Plain, A. Bouchoule, C. Laure, and J. P. Boeuf, Phys. Rev. A **46**, 7923 (1992); J. P. Boeuf, *ibid.* **46**, 7910 (1992).
[17] H. Thomas, G. E. Morfill, V. Demmel, J. Goree, B. Feuerbacher, and D. Mohlmann, Phys. Rev. Lett. **73**, 652 (1994).
[18] A. Melzer, A. Homann, and A. Piel, Phys. Rev. E **53**, 2757 (1996).
[19] L. Jeng-Mei, J. Wen-Tau, H. Ju-Wang, H. Zen-Hong, and I. Lin, Plasma Phys. Controlled Fusion **41**, A47 (1999).
[20] G. Praburam and J. Goree, Phys. Plasmas **3**, 1212 (1996); J. Goree, G. E. Morfill, V. N. Tsytovich, and S. V. Vladimirov, Phys. Rev. E **59**, 7055 (1999).

[21] V. E. Fortov, A. P. Nefedov, O. S. Vaulina, A. M. Lipaev, V. I. Molotkov, A. A. Samaryan, V. P. Nikitski, A. I. Ivanov, S. F. Savin, A. V. Kalmykov, A. Ya. Solov'ev, and P. V. Vinogradov, Sov. Phys. JETP **87**, 1087 (1998).
[22] G. E. Morfill, H. M. Thomas, U. Konopka, H. Rothermel, M. Zuzic, A. Ivlev, and J. Goree, Phys. Rev. Lett. **83**, 1598 (1999).
[23] A. P. Nefedov, G. E. Morfill, V. E. Fortov, H. M. Thomas, H. Rothermel, T. Hagl, A. V. Ivlev, M. Zuzic, B. A. Klumov, A. M. Lipaev, V. I. Molotkov, O. F. Petrov, Y. P. Gidzenko, S. K. Krikalev, W. Shepherd, A. I. Ivanov, M. Roth, H. Binnenbruck, J. A. Goree, and Y. P. Semenov, New J. Phys. **5**, 33.1 (2003).
[24] J. Goree, Plasma Sources Sci. Technol. **3**, 400 (1994).
[25] B. Bernstein and I. N. Rabinowitz, Phys. Fluids **2**, 112 (1959); G. Laframboise, Ph.D. thesis, University of Toronto, Toronto, 1966.
[26] H. M. Mott-Smith and I. Langmuir, Phys. Rev. **28**, 727 (1926).
[27] J. P. Bouef and C. Punset, in *Dusty Plasmas: Physics, Chemistry and Technological Impacts in Plasma Processing*, edited by A. Bouchoule, (Wiley, Chichester, 1999).
[28] B. T. Draine and E. E. Salpeter, Astrophys. J. **231**, 77 (1979); B. T. Draine, B. Sutin, *ibid.* **320**, 803 (1987); J. C. Weingartner and B. T. Draine, Astrophys. J., Suppl. Ser. **134**, 263 (2001).
[29] M. Rosenberg and D. A. Mendis, IEEE Trans. Plasma Sci. **233**, 177 (1995); J. Pavlu, Z. N. Nemecek, J. Šafrankova, and I. Cermak, *ibid.* **32**, 607 (2004).
[30] J. Berndt, E. Kovačević, V. Selenin, I. Stefanović, and J. Winter, Plasma Sources Sci. Technol. **15**, 18 (2006).
[31] A. V. Phelps and Z. Lj. Petrović, Plasma Sources Sci. Technol. **8**, R21 (1999).
[32] E. Kovačević, I. Stefanović, J. Berndt, and J. Winter, J. Appl. Phys. **93**, 2924 (2003).
[33] I. Stefanović, E. Kovačević, J. Berndt, Y. Pendelton, and J. Winter, Plasma Phys. Controlled Fusion **47**, A179 (2005).
[34] B. Tomčik, A. Jelenak, M. Mitrović, and Z. Lj. Petrović, Diamond Relat. Mater. **4**, 1126 (1995).
[35] I. Stefanović, E. Kovačević, J. Berndt, and J. Winter, New J. Phys. **5**, 39.1 (2003).
[36] G. Malović, A. Strinić, S. Živanov, D. Marić, and Z. Lj. Petrović, Plasma Sources Sci. Technol. **12**, S1 (2003).
[37] S. Živanov, J. Živković, I. Stefanović, S. Vrhovac, and Z. Lj. Petrović, Eur. Phys. J.: Appl. Phys. **11**, 59 (2000).
[38] I. Stefanović and Z. Lj. Petrović, Jpn. J. Appl. Phys., Part 1 **36**, 4728 (1997).
[39] M. J. Druyvesteyn and F. M. Penning, Rev. Mod. Phys. **12**, 87 (1940).
[40] A. A. Kruithof, Physica (Amsterdam) **7**, 519 (1940).
[41] M. Radmilović, Z. Lj. Petrović, and B. Radjenović, in *Proceedings of the Joint Conference of 16th Escampig and 5th ICRP, Grenoble, 2002*, edited by N. Sadeghi and H. Sugai, 2002, Vol. 2 (TB4), p. 261.
[42] M. Radmilović and Z. Lj. Petrović, Eur. Phys. J.: Appl. Phys. **11**, 35 (2000).
[43] S. Bzenić, Z. M. Raspopović, S. Sakadžić, and Z. Lj. Petrović, IEEE Trans. Plasma Sci. **27**, 78 (1999).
[44] T. Makabe and Z. Lj. Petrović, *Plasma Electronics: Applications in Microelectronic Device Fabrication* (Taylor and Francis, CRC, New York, 2006).
[45] C. Cui and J. Goree, IEEE Trans. Plasma Sci. **22**, 151 (1994).
[46] M. Radmilović-Radjenović, J. K. Lee, F. Iza, and G. Y. Park, J. Phys. D **38**, 950 (2005).
[47] R. R. Newton, Phys. Rev. **73**, 1122 (1948).
[48] R. A. Baragiola, in *Low Energy Ion-Surface Interactions*, edited by J. W. Rabalais (Wiley, New York, 1994).
[49] R. H. Good and E. W. Mller, in *Encyclopedia of Physics, Vol. XXI, Electron-Emission Gas Discharges I*, edited by S. Flgge (Springer-Verlag, New York, 1988).
[50] J. Bonard, R. Gaal, S. Garaj, L. Thien-Nga, L. Forr, K. Takahashi, F. Kokai, M. Yudasaka, and S. Iijima, J. Appl. Phys. **91**, 10107 (2002).
[51] A. A. Sickafoose, J. E. Colwell, M. Horanyi, and S. Robertson, Phys. Rev. Lett. **84**, 6034 (2000).
[52] Z. Sternovsky, M. Horanyi, and S. Robertson, J. Vac. Sci. Technol. A **19**, 2533 (2001).
[53] E. Stoffels (private communication).
[54] Z. Lj. Petrović, Ph.D. thesis, Australian National University, 1985.
[55] J. Lambert, G. de Loubens, C. Guthmann, M. Saint-Jean, and T. Melin, Phys. Rev. B **71**, 155418 (2005).
[56] J. U. Andersen, E. Bonderup, and K. Hansen, J. Phys. B **35**, R1 (2002).
[57] R. A. Baragiola, E. V. Avlonso, J. Ferron, and A. Oliva-Florio, Surf. Sci. **90**, 240 (1979).
[58] S. T. Lai, IEEE Trans. Plasma Sci. **31**, 1118 (2003).